JOURNAL OF SOLID STATE CHEMISTRY 43, 140–150 (1982)

A Pressure-Induced Nonlayered Structure of Indium Monoselenide

YOUSUKE WATANABE, HIROSHI IWASAKI,* NORITAKA KURODA, AND YUICHIRO NISHINA

The Research Institute for Iron, Steel and Other Metals, Tohoku University, Sendai 980, Japan

Received October 21, 1981; in revised form February 19, 1982

An X-ray diffraction study was made on a new polymorphic phase of InSe obtained by heating a layered crystal of the 3R(γ) polytype under pressures of 40 and 50 kbar and by quenching to ambient conditions. An analysis of the diffraction intensity data collected on precession and Debye photographs gave a monoclinic structure (space group C_{2h}^{1}) with four molecules in a unit cell. Upon transformation, new, short interatomic distances characteristic of covalent bonding are formed between indium and selenium atoms that were originally located in the adjacent layers. The structure is regarded as a modified version of the nonlayered InS-type structure. In the real structure of the high-pressure phase, however, there is a small amount of disorder in the orientation of the In–In bonds. Discussion is given on the reconstructive, layer–nonlayer transformation of InSe.

Introduction

III–VI compounds such as GaS, GaSe, and InSe are known to form a family of layered semiconductors and their structure is described as a regular stacking of layers, each consisting of hexagonal sublayers bound in the order X–M–M–X (M representing the cation and X the anion) as shown in Fig. 1. There are several ways in which the layers are stacked and Fig. 2a shows the one frequently observed and designated as a 3R or γ polytype. It is a projection of the structure onto the (10 · 0) plane and the fractional numbers attached to the atoms represent their elevation from the projection plane. Besson (*1*) reported, on the basis of Raman scattering measurements, that when GaS and GaSe are subjected to pressure, the restoring force associated with the interlayer van der Waals bonding increases, while the intralayer force remains almost unchanged. This fact suggests that covalent bonding could be formed between the layers if the pressure reached about 120 kbar. Nevertheless, no experimental evidence of the conversion of the bonding has been reported on these layered compounds.

The present authors (Y.N. and N.K.) (*2*) have carried out a calculation of the energy spectrum of long-wavelength optical phonons in the III–VI compounds on the basis of the deformation dipole model and suggested that shear mode phonons induce an instability of the layered structure if the molecular polarizability is in a critical region. While GaS and GaSe lie in molecular polarizability far from the region, InSe lies very close to and InS just in the region. In fact, the layered structure of GaS and GaSe is stable as mentioned above, whereas InS

* To whom correspondence should be addressed.

0022-4596/82/080140-11$02.00/0

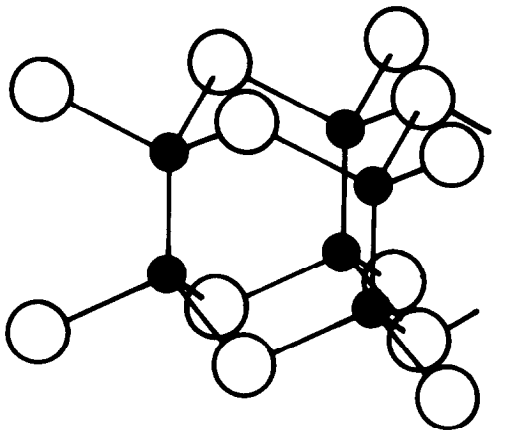

FIG. 1. Atomic arrangement in a unit layer of the III–VI compounds. Small and large circles represent the cation and anion, respectively.

is known to have a nonlayered structure (*3*), which can be obtained by introducing a periodic shear distortion into the GaS-type structure. This fact suggests that the layered structure of InSe may transform into the structure of InS type, if the condition for the instability is satisfied. These suggestions lead us to pay attention to the work of Vessoli (*4*), reporting that the structure of InSe was changed if the powdered specimen was held to 250°C for 20 hr while being subjected to a pressure of 40 kbar. Though X-ray diffraction data on quenched specimens were given (*4*), no structural investigation was conducted. However, the high-pressure phase was reported to be of a reconstructive nature and was suggested to be related to some kind of polytypism.

The present work was undertaken to confirm the reported pressure-induced transformation in InSe and to determine the structure of the high-pressure modification. The results obtained, mainly by means of X-ray diffraction, show that the structure is indeed a modified version of the InS-type structure, having strong interlayer covalent bonding. This is the first example of reconstructive, layer–nonlayer transformation found in semiconducting compounds.

Experimental Procedures

Single crystals of InSe were grown by the Bridgman method from stoichiometric composition of indium and selenium. Samples were obtained by cleaving the single-crystal ingot. The polytype of these samples was identified with 3R(γ) from X-ray precession photographs taken with the incident beam normal and parallel to the plane of the crystal flake.

A Bridgman-anvil-type apparatus equipped with an internal heater of tantalum foils was used for high-pressure experiments. Several pieces of the single-crystal samples were compressed between a pair of tung-

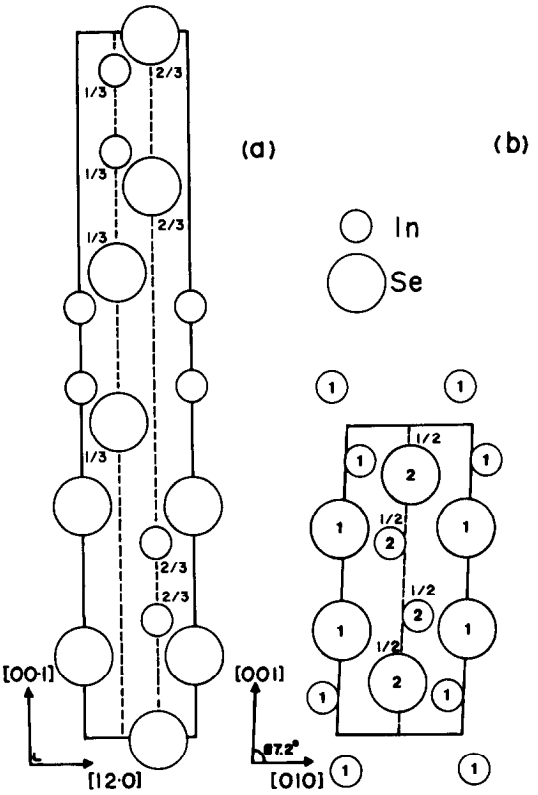

FIG. 2. Structure of (a) InSeI (3R(γ) polytype) and (b) InSeII projected onto the (10 · 0) and (100) plane, respectively. Fractional numbers attached to the atoms represent their elevation from the plane of projection.

sten carbide anvils with boron nitride as the pressure transmitting medium and pyrophyllite as the gasket material. In some runs, powdered samples prepared by crushing the crystal flake were compressed. Details of the high-pressure cell and the method of pressure and temperature calibration were described elsewhere (*5*).

The pressure was first increased to a predetermined value and then the temperature was raised. The samples were held at the pressure and temperature for several days. Then, the temperature was rapidly lowered by switching off the heater current and the pressure was released subsequently.

A series of precession photographs was taken from the single-crystal sample thus quenched to ambient conditions using filtered Mo$K\alpha$ and Cu$K\alpha$ radiation. If the X-ray beam was incident normal to the crystal flake, diffraction patterns with moderate contrast were obtained. On the other hand, a heavy absorption of X rays was observed if the beam was incident parallel to the plane of the flake. As expected, the sample was no longer in a single-crystal form after transformation had taken place. This crystallographic degradation of the sample, together with the remarkable anisotropy in absorption, did not permit a full utilization of the precession photographs for structure determination. The precession technique, however, gave valuable information on the crystal symmetry, unit cell sizes, and orientation relationship between the crystal lattices of the low-pressure and the high-pressure phases. We therefore resorted to the intensity measurement of diffraction lines on Debye photographs, taken using filtered Cu$K\alpha$ radiation from the powdered samples that were quenched in the same way, for the refinement of atomic positional parameters. A microphotometer was used to measure the intensity of reflections on X-ray films, the visual estimation technique also being used as an auxiliary method for weak reflections.

Structure Determination of InSeII

(*a*) *Characteristics of Intensity Distribution and Unit Cell Sizes*

Figure 3 shows an X-ray diffraction photograph of the powdered InSe sample maintained at 40 kbar and 250°C for 2 days. Holding at higher temperatures or at higher pressures gave essentially the same diffrac-

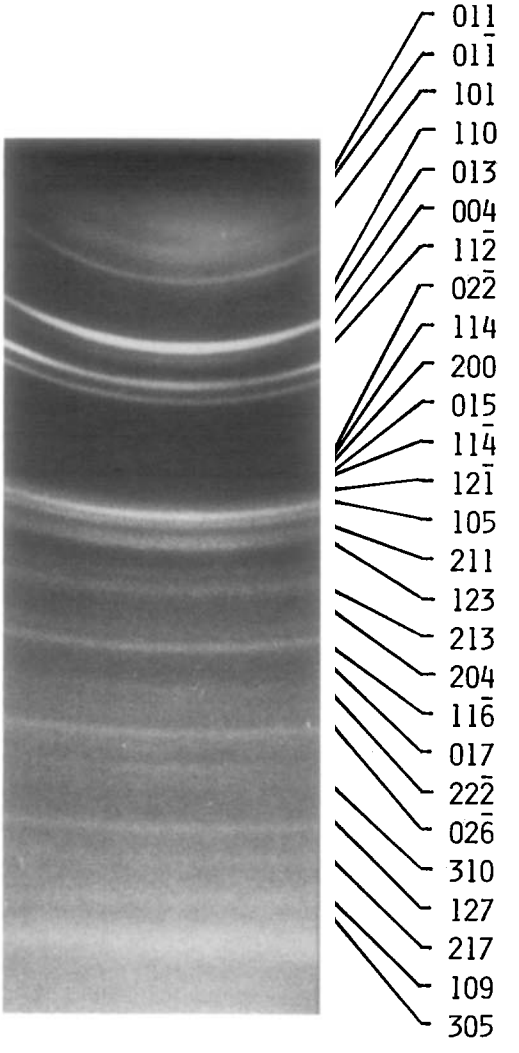

FIG. 3. X-ray Debye photograph of InSeII. Indices are assigned on the basis of the monoclinic unit cell. Filtered Cu$K\alpha$ radiation.

tion pattern, except a small variation from sample to sample in the d values of some diffraction lines. A remarkable feature common to all samples is the existence of three strong reflections with d values of 3.07, 2.75, and 2.05 Å. This feature of the diffraction pattern is in agreement with that reported in Vessoli's paper (*4*). The variation in the d values, which was also observed by Vessoli, is probably caused by a small difference in the degree of completion of the transformation. Hereafter, we designate the phase obtained by high-pressure heating as InSeII in order to distinguish from the phase InSeI having the layered structure.

Any attempt to index the diffraction lines of the pattern shown in Fig. 3 in terms of a cubic, hexagonal, or tetragonal crystal system has been unsuccessful.

Figure 4b shows a precession photograph of the single crystal-like InSeII sample recovered from holding at 50 kbar and 350°C for 3 days. For the sake of comparison, a precession photograph of the InSeI single crystal is shown in Fig. 4a. This represents a section of the reciprocal lattice parallel to the basal plane of the layered structure, and the photograph in Fig. 4b was taken with the same incident beam direction to the crystal flake as that in Fig. 4a. The sixfold symmetry seen in the pattern of InSeI is completely lost in the pattern of InSeII. Distribution of the diffraction spots in Fig. 4b suggests an orthorhombic or lower symmetry for InSeII. It should be noted that the diffraction pattern does not correspond to that of a single-crystal form but rather to that of a crystal containing several orientation variants. Besides, the diffraction spots are somewhat diffuse, indicating lattice distortion introduced upon transformation. In spite of these degradations of crystallinity, it is possible to index many of the diffraction spots in Fig. 4b in terms of a centered rectangular lattice with $a = 4.1$ and $b = 4.6$ Å.

The precession photographs taken to explore the sections of the reciprocal lattice perpendicular to the plane of Fig. 4b show ill-defined diffraction spots, some of them arcing and others spreading. It is possible to choose the third axis, c, 11.0 Å in length,

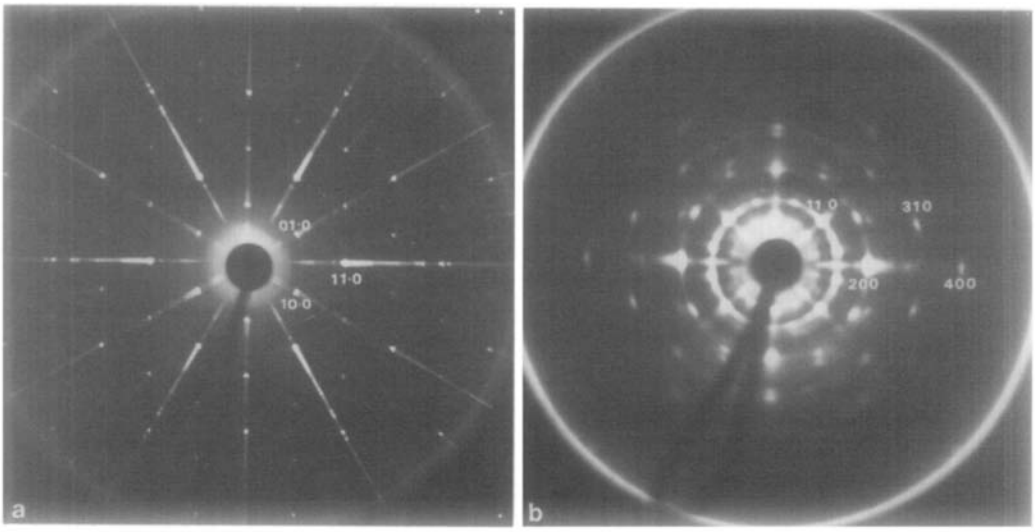

FIG. 4. X-ray precession photograph of (a) InSeI and (b) InSeII. X-ray beam is incident normal to the basal plane of the layered structure (a) and parallel to the corresponding direction (b). Filtered Mo$K\alpha$ radiation. 10 · 0 and 01 · 0 are the spurious spots due to arcing.

nearly normal to the a–b plane and to allot the three-dimensional indices to many of the diffraction spots. Then the spots corresponding to the aforementioned three diffraction lines have the indices 110, 004, and 200. This fact strongly suggests that the structure of InSeII is very similar to the orthorhombic InS structure, as first expected, because the latter structure also gives large amplitudes of X-ray diffraction for the reflections having these indices (*6*). The InS structure is shown in Fig. 5. However, indexing of the diffraction spots and diffraction lines in terms of an orthorhombic lattice with $a = 4.1$, $b = 4.6$, and $c = 11.0$ Å is not perfectly convincing. Rather, satisfactory results can be obtained if the crystal lattice of InSeII is assumed to be monoclinic with the angle α between the b and c axes slightly deviating from 90°. The lattice parameters a, b, c, and α were then refined using the selected d values of sharp diffraction lines in the Debye photograph and a fair agreement between the observed and calculated interplanar spacings was obtained as shown in Table I. The parameters refined for the sample held at 40 kbar and 250°C for 2 days are $a = 4.11 \pm 0.01$, $b = 4.61 \pm 0.01$, $c = 11.02 \pm 0.02$ Å, and $\alpha = 87.2 \pm 0.3°$. As will be shown later, the real structure of InSeII contains a small amount of disorder and these values, especially that of α, should be regarded as the average ones.

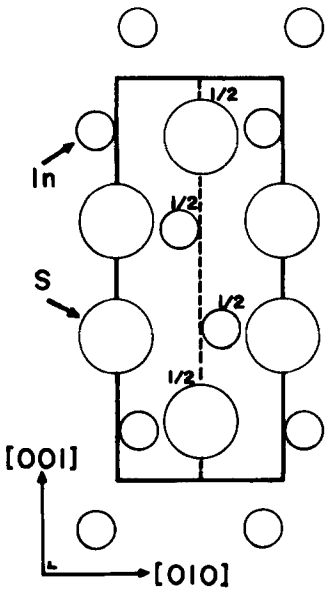

FIG. 5. Structure of InS projected onto the (100) plane.

(*b*) *Structure of InSeII*

The next step is to determine an atomic arrangement in the monoclinic unit cell. The systematic extinction of the $hk0$-type reflections with $h + k = 2n + 1$ observed for InSeII again suggests the structural similarity between InSeII and InS. Four In atoms and four Se atoms are tentatively disposed just as In and S atoms are in the InS structure and the unit cell is distorted in order to become monoclinic. The intensities of the reflections are then calculated and are in fair agreement with those observed for the $hk0$- and $h0l$-type reflections but not for the $0kl$- and general hkl-type ones. An appreciable improvement in the correspondence between the calculated and observed intensities can be obtained if the orientation of the In–In bonds in the InS structure is changed so that they are all tilted in the same direction, as shown in Fig. 2b. This structure model for InSeII, hereafter called an ideal structure model, belongs to the space group $C_{2h}^{1} - P2/m$ and the atomic positional parameters determined using the intensity data collected on the Debye photograph are as follows.

Atom	Site	x	y	z
In(1)	$2m$	0	$-\frac{1}{8}$	$\frac{3}{26}$
In(2)	$2n$	$\frac{1}{2}$	$\frac{5}{8}$	$\frac{19}{26}$
Se(1)	$2m$	0	0	$\frac{9}{26}$
Se(2)	$2n$	$\frac{1}{2}$	$\frac{1}{2}$	$\frac{4}{26}$

There still remains a discrepancy between the calculated and observed intensities for several reflections, such as 101 and

TABLE I

CALCULATED AND OBSERVED INTERPLANAR SPACINGS, d, AND INTENSITIES, I, OF InSeII

h	k	l	d_c (Å)	d_o (Å)	I_c	I_o	h	k	l	d_c (Å)	d_o (Å)	I_c	I_o
0	0	2	5.503	5.50	5.1	6	0	1	−7	1.466		0.4	
0	1	1	4.324	4.324	9.9	6	2	2	−2	1.465	1.460	2.3	8
0	1	−1	4.176	4.17	1.6	2	1	2	−5	1.453		0.0	
1	0	1	3.850	3.849	18.9	17	2	1	5	1.442		3.0	
0	1	2	3.620		0.0		0	3	3	1.441	1.44	0.5	2b
0	1	−2	3.450		0.0		1	3	0	1.438		0.0	
1	1	0	3.066	3.065	56.4	100	2	1	−5	1.414		0.9	
0	1	3	2.940	2.936	9.5	6	1	3	2	1.407		0.2	
0	1	−3	2.803		1.1		0	2	−6	1.402	1.40	1.2	4b
0	0	4	2.752	2.753	55.0	55	0	3	−3	1.392		0.1	
1	0	3	2.737		0.5		1	3	−2	1.376		0.7	
1	1	2	2.716		8.3		0	0	8	1.376	1.37	1.7	2b
1	1	−2	2.642	2.642	21.5	25	2	0	6	1.369		0.6	
0	2	0	2.302	2.30	0.9	2	3	0	1	1.360		0.8	
0	2	2	2.162	2.16	1.7	2	2	2	4	1.358		0.1	
0	2	−2	2.088	2.076	4.0	20b	2	2	−4	1.321		0.1	
1	1	4	2.082		10.7		3	1	0	1.313	1.308	3.6	8
2	0	0	2.055	2.048	33.3	40	1	3	4	1.299		0.0	
0	1	5	2.025	2.015	5.0	20b	0	3	5	1.289		0.0	
1	1	−4	2.016		12.4		3	0	3	1.283		0.1	
1	2	1	1.991		0.0		3	1	2	1.281		0.6	
1	2	−1	1.961		2.1		3	1	−2	1.273		1.8	
0	1	−5	1.949	1.949	1.4	30b	1	1	8	1.271	1.267	0.1	6b
1	0	5	1.941		23.2		1	2	7	1.265		1.4	
2	0	2	1.925		0.6		1	1	−8	1.240		0.7	
2	1	1	1.856	1.848	2.0	6	0	3	−5	1.231		0.0	
2	1	−1	1.844		0.3		2	3	1	1.227		0.1	
0	0	6	1.834		0.9		2	3	−1	1.217	1.22	0.2	6b
0	2	4	1.810		0.1		2	1	7	1.217		1.3	
1	2	3	1.794	1.792	4.6	11b	1	2	−7	1.213		0.2	
1	2	−3	1.731		0.0		0	2	8	1.207		0.0	
0	2	−4	1.725		0.2		0	1	9	1.197		1.3	
2	1	3	1.684	1.681	3.5	3	2	2	6	1.196		0.1	
2	1	−3	1.657		0.4		2	1	−7	1.194		0.3	
2	0	4	1.647	1.642	22.3	17	3	1	4	1.192		1.3	
1	1	6	1.597		0.3		2	3	3	1.180		0.5	
1	1	−6	1.552	1.550	4.8	5	3	1	−4	1.179		1.6	
2	2	0	1.533		0.5		3	2	1	1.174		0.0	
0	3	1	1.530		0.2		1	0	9	1.172		7.2	
1	2	5	1.516		0.2		3	2	−1	1.168	1.17	0.3	20b
0	3	−1	1.511	1.51	0.3	3b	0	1	−9	1.168		0.9	
0	1	7	1.510		1.6		3	0	5	1.163		3.2	
2	2	2	1.489		1.0		2	2	−6	1.158		1.1	
0	2	6	1.470		0.1		1	3	6	1.158		0.0	
1	0	7	1.469		0.1		0	2	−8	1.156		0.0	

Note. Existence of disorder in the In–In bond orientation is taken into account in the calculation. I is normalized to that of the 004 reflection. $I_c = |F|^2 \cdot LP \cdot j$. b represents broadening.

013, and it is not possible to remove it as long as the positional parameters are varied within the framework of the space group C_{2h}^{1}. However, introduction of a small amount of disorder in the orientation of the In–In bonds into the ideal structure model is shown to decrease the calculated intensity of the particular reflections and thus get an overall agreement. Before going into the description of the above disorder, a general structural feature of InSeII should be discussed. The precession photographs taken before and after high-pressure heating show that the (001) plane of the InSeII structure is formed parallel to the basal plane of the original layered structure, as shown in Fig. 2. This orientation relationship gives a clue for deducing an atomistic mechanism of the transformation. It can be seen that the InSeII structure retains the framework of the original layers. For instance, In(2) and Se(1) atoms in Fig. 2b form a sheet of the original layer. It is worth noting that the interatomic distance between Se atoms that were originally located in the same layer is decreased by as much as 35% and the In–In bonds, which were directed parallel to the [00 · 1] direction of the layered structure, are titled in the InSeII structure. A remarkable contraction is found for the interatomic distance between In and Se atoms, which were originally located in the adjacent layers and separated by the distance 4.28 Å. That distance in InSeII becomes 2.61 Å, which is typical of *covalent* bonding between a pair of In and Se atoms. In the InSeI structure, the bonding between the layers is due to a weak van der Waals interaction between Se atoms, but in the InSeII structure it is replaced by strong covalent bonding between In and Se atoms. It is to be noted that each In atom still has two other Se atoms as the nearest neighbors in the same original layer.

Comparison of the unit cell volumes of InSeI and InSeII, 346.0 (six molecules) and 208.5 Å^3 (four molecules), indicates that the latter structure is 9.6% denser than the former and this densification derives mainly from the decrease in the distances between Se atoms and between In and Se atoms as mentioned above.

(*c*) *Disorder in the Structure of InSeII*

The structure of InSeII is regarded as a modified version of the InS structure. The major difference in the two structures exists in the orientation of the In–In bonds. As far as the nearest-neighbor distances are concerned, there is no significant difference in the arrangements of cations and anions and, therefore, there is the opportunity for the In–In bonds in the InSeII structure to take the InS-type orientation. The ideal structure model of InSeII gives stronger intensity to the 013 reflection than the 101 reflection, being contrary to the observation. On the other hand, the InS-type atomic arrangement gives very weak intensity to the 013 reflection. An assumption is made that the real InSeII structure contains partially In–In bonds with the InS-type orientation, which will remove the remaining discrepancy for these reflections. Our problem is now how to calculate the intensities of the reflections from the crystal containing such a type of disorder. For this purpose, a diffraction theory originally developed by Kakinoki and Komura (*7*) is used.

We consider the InSeII structure, Fig. 2b, as a stacking of the two kinds of block sheets consisting of In(1) and Se(2) atoms and of In(2) and Se(1) atoms. These block sheets are denoted by A and A′, respectively, so that the ideal structure model is described as AA′AA′AA′ . . ., A and A′ differing from each other by the translation $(\frac{1}{2})(a + b)$. Next the block sheets B and B′ are defined, in which the In–In bond takes an alternative inclination. The stacking sequence BA′BA′BA′ . . . or B′AB′AB′A . . . corresponds to the InS-like atomic arrangement. Two parameters μ and ν are introduced which represent the sequence

probabilities of the four kinds of block sheets as shown in Table II. We calculated the intensities of reflections of the partially disordered InSeII crystal and determined the values of μ and ν using the intensity data collected on the Debye photograph by a least-squares refinement technique. The atomic positional parameters in the block sheet were simultaneously refined. Details in the method of the calculation are given in the Appendix.

The results are $\mu = 0.003$ and $\nu = 0.66$. That is, starting from the normal sequence of block sheets, AA'AA'AA' . . ., there is a probability of 0.003 of a B (or B') block sheet coming after A' (or A) and, once it occurs, there is a probability of 0.66 of returning to the normal sequence. Although the μ value is small, introduction of the disorder has greatly improved the correspondence between the observed and calculated intensities of reflections. In Table I the calculated intensities are compared with the observed ones for the InSeII sample recovered from holding at 40 kbar and 250°C for 2 days. Prolonged high-pressure heating would be necessary to get the ideal InSeII structure with $\mu = 0$ and $\nu = 1$. As a result of the refinement, the atomic positional parameters, expressed in terms of the monoclinic lattice, are determined to be as follows:

Atom	Site	x	y	z
In(1)	2m	0	−0.121	0.116
In(2)	2n	½	0.621	0.384
Se(1)	2m	0	0.018	0.340
Se(2)	2n	½	0.482	0.160

These parameters should be regarded as those of the part of the structure where the normal sequence of block sheets extends. The volume fraction of this part is large, as suggested by the results of the disorder analysis.

Using the refined atomic positional parameters, the principal interatomic distances in InSeII are calculated and shown in Table III. Those between the atoms located in the adjacent block sheets are the values averaged over the four kinds of sequence with the weights of their probability μ and ν. For comparison purpose, the corresponding distances in InSeI (*8*) are also shown.

TABLE II

SEQUENCE PROBABILITIES OF THE FOUR KINDS OF BLOCK SHEETS IN InSeII

	A	B	A'	B'
A			$1 - \mu$	μ
B			ν	$1 - \nu$
A'	$1 - \mu$	μ		
B'	ν	$1 - \nu$		

Discussion

The structures of InSeI (3R(γ) polytype) and InSeII (ideal structure) are compared in Fig. 2. As mentioned above, the (001) plane of the latter structure is formed parallel to the basal plane of the former structure. Hence the transformation must proceed

TABLE III

PRINCIPAL INTERATOMIC DISTANCES IN InSeI AND InSeII

	InSeI[a] (Å)	InSeII[b] (Å)
Intralayer		
In–In	2.770	2.77 (0.03)
Se–Se	5.281	3.53 (0.03)
In–Se	2.626	2.79 (0.02)
Interlayer		
In–In	6.009 7.220	3.73 (0.03) 5.11 (0.03)
Se–Se	3.814 5.528	3.46 (0.03) 3.91 (0.04)
In–Se	4.281	2.61 (0.03)

[a] After Rigoult *et al.* (*8*).

[b] Due account is taken for the presence of disorder in the orientation of In–In bonds.

first by relative displacements of the layers themselves as well as of the sublayers of InSeI. The displacements of the layers change the stacking sequence from the 3R type to the 2H type. The displacements of the sublayers change the internal structure of the layer and induce the tilting of the In–In bonds with an attendant decrease in the layer thickness. The disorder in the bond orientation is introduced in this step. Then, the extended In–Se bonds within the layer are broken up to reconstruct new interlayer In–Se bonds. The reconstruction can occur with respect to one of three equivalent In–Se bonds per molecular unit so that at least three orientation variants may possibly coexist in InSeII. The presence of the orientation variants was actually observed, although they are not necessarily equal in the volume fraction. Formation of the strong In–Se bonds now greatly reduces the interatomic distances in the [001] direction. The shearing deformation of the (001) plane from hexagonal to rectangular arrangement of coplanar atoms then follows and leads to the InSeII structure.

It is to be noted that not only compression but also heating of the sample is required to induce the transformation in InSe. Moreover, InSeII remains quite stable, as long as it is kept at ambient conditions. Reversion to the original layered structure was observed after heating the transformed crystal at 500°C for 1 day. These facts imply that the potential barrier lying between equilibrium positions of atoms in the low- and high-pressure structures is much higher than the thermal energy corresponding to room temperature. This is in contrast to the reversible transformations found in the III–V compounds (*9*).

Raman scattering measurements were performed on the InSe sample before and after the high-pressure high-temperature treatment (*10*). The transformation removes the degeneracy of E^2 and E^3 modes in InSeI and shifts the frequencies of A_1^2 and A_1^3 modes. The remarkable blue shift of the A_1^2 peak provides clear evidence of the formation of covalent bonding between In and Se atoms which were bonded in InSeI across the adjacent layers by the weak van der Waals forces.

Finally, we would like to mention the polytypism of InSeI. As argued in the preceding section, we almost always obtained the 3R(γ) polytype if the crystals were grown by the Bridgman method. Occasionally a hexagonal polytype was found in the form of the mixture with the 3R(γ) polytype. Inoue (*11*) also found a hexagonal polytype in crystals grown by the vapor transport method and identified it as the 2H(ϵ). To the authors' knowledge, the 2H(β) polytype has never been reported in InSe. The hexagonal polytype can be definitely distinguished from the 3R(γ) by Raman scattering spectra, because the *rigid layer mode* is allowed in both 2H polytypes but it is forbidden in the 3R(γ), as has been clearly demonstrated by the present authors (*12, 13*). Recently Carlone *et al.* (*14*) also measured the Raman scattering of InSe. On the basis of the number of Raman lines observed, they claimed that the crystal grown by the Bridgman method was of 2H(β) polytype. Their conclusion, however, is quite questionable because (1) their group theoretical analysis of the 3R(γ) polytype is based on a nonprimitive unit cell to give the wrong number of Raman active phonon modes, and (2) the distinction between 2H(ϵ) and 2H(β) polytypes of a given crystal by means of Raman scattering measurements relies only on the difference in the very weak interlayer interaction and therefore is not nearly conclusive.

Appendix: Calculation of the Intensity of Reflections from Partially Disordered InSeII Crystal

The structure factor of the A- and B-type

block sheets are written as follows

$$F_A = 2f_{In}\exp\left\{-B_{In}\frac{\sin^2\theta}{\lambda^2}\right\}\cos 2\pi(kY_{In} + lZ_{In}) + 2f_{Se}\exp\left\{-B_{Se}\frac{\sin^2\theta}{\lambda^2}\right\}\cos 2\pi\left(\frac{h}{2} + kY_{Se} + lZ_{Se}\right)$$

and

$$F_B = 2f_{In}\exp\left\{-B_{In}\frac{\sin^2\theta}{\lambda^2}\right\}\cos 2\pi(-kY_{In} + lZ_{In}) + 2f_{Se}\exp\left\{-B_{Se}\frac{\sin^2\theta}{\lambda^2}\right\}\cos 2\pi\left(\frac{h}{2} - kY_{Se} + lZ_{Se}\right),$$

where f_{In} and f_{Se} represent the atomic scattering factors of In and Se atoms, and B_{In} and B_{Se} their temperature factors. Y_{In}, Z_{In}, Y_{Se}, and Z_{Se} are the atomic positional parameters. For the sake of simplicity, we have chosen the third axis to be normal to the a–b plane and have the length equal to the thickness of the block sheet. In order to take into account the monoclinic distortion of the structure, we introduce a vector **u** parallel to the b axis, by which a block sheet is displaced when it is stacked, as shown in Fig. A1. In cases where the block sheet having different bond orientation is stacked, the relative displacement is v.

Then the so-called reduced P matrix (7) can be written as

$$P = \begin{pmatrix} (1-\mu)\epsilon_{11} & \mu\epsilon_{12} \\ \nu\epsilon_{21} & (1-\nu)\epsilon_{22} \end{pmatrix}$$

with

$$\epsilon_{11} = \exp\left\{2\pi i\left(\frac{h+k}{2} + ku\right)\right\},\quad \epsilon_{12} = \exp\left\{2\pi i\left(\frac{h+k}{2} + kv\right)\right\},$$

$$\epsilon_{21} = \exp\left\{2\pi i\left(\frac{h+k}{2} - kv\right)\right\},\quad \epsilon_{22} = \exp\left\{2\pi i\left(\frac{h+k}{2} - ku\right)\right\}.$$

Following the procedures usually adopted in the calculation of scattering intensity from the faulted crystals, the intensity formula is expressed in the form

$$I(hkl) = ND(hkl) + H(hkl;N),$$

where N is the number of the block sheets in the coherent region and

$$D(hkl) = \sum_{i=1}^{2}\left(\frac{b_i}{1-y_i} + \text{complex conj.}\right) - B_o,$$

$$H(hkl;N) = \sum_{i=1}^{2}\left\{\frac{b_i y_i(y_i^N - 1)}{(1-y_i)^2} + \text{complex conj.}\right\},$$

with

$$y_1 = \tfrac{1}{2}(-A_1 + (A_1^2 - 4A_2)^{1/2}),$$
$$y_2 = \tfrac{1}{2}(-A_1 - (A_1^2 - 4A_2)^{1/2}),$$
$$b_1 = \frac{y_1B_0 - B_1}{y_1 - y_2},$$
$$b_2 = -\frac{y_2B_0 - B_1}{y_1 - y_2},$$
$$A_1 = -\{(1-\mu)\epsilon_{11} + (1-\nu)\epsilon_{22}\}e^{-i2\pi l},$$
$$A_2 = \{(1-\mu)(1-\nu)\epsilon_{11}\epsilon_{22} - \mu\nu\epsilon_{12}\epsilon_{21}\}e^{-I4\pi l},$$

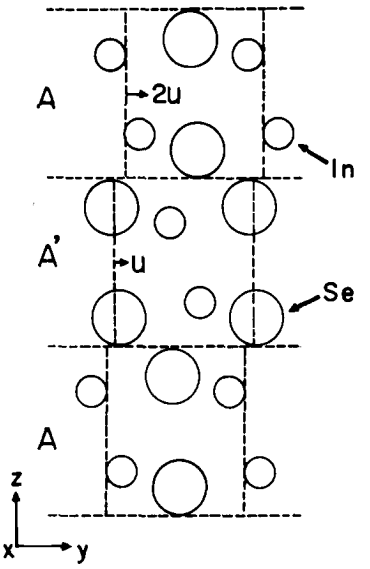

FIG. A1. InSeII structure regarded as a stacking of the block sheets.

$$B_0 = W_A F_A^2 + W_B F_B^2,$$

$$B_1 = \{W_A F_A^2(1 - \mu)\epsilon_{11} + W_B F_A F_B \nu \epsilon_{21} + W_A F_A F_B \mu \epsilon_{12} + W_B F_B^2(1 - \nu)\epsilon_{22}\} e^{-i2\pi l},$$

$$W_A = \nu/(\mu + \nu),$$

$$W_B = \mu/(\mu + \nu).$$

The term $D(hkl)$ is the intensity of diffuse scattering and $H(hkl;N)$ is the intensity corresponding to that of the Bragg reflection. The parameters μ, ν, Y_{In}, Z_{In}, Y_{Se}, and Z_{Se} were determined by a least-squares method in which modified Marquardt numerical analytical method was used. The sum of $H(hkl;N)$ and a part of $ND(hkl)$ located beneath the Bragg peak is taken as the calculated intensity of the hkl reflection and compared with the observed intensity of the reflection recorded on the Debye photograph. The parameter u is chosen to be $0.058 \cdot b$ so that an average inclination angle of the z axis of faulted crystal is equal to the monoclinic angle α, while our disorder model makes v no relevance to the angle α and v is put to be zero. The parameter N is shown to have no significant influence on the calculated intensity within the range 500–2000 and we put it to be 2000. The parameters thus determined are $\mu = 0.003$, $\nu = 0.66$, $Y_{In} = -0.115$, $Z_{In} = 0.232$, $Y_{Se} = 0.490$, and $Z_{Se} = 0.320$. These parameters can be transformed into those referred to the monoclinic lattice and are given in the text.

Acknowledgments

The technical assistance of Dr. W. K. Wang in high-pressure experiments is greatly acknowledged. Least-squares refinement was carried out on the program SALS written by Nakagawa and Koyanagi.

References

1. J. M. Besson, *Nuovo Cimento B* **38,** 478 (1977).
2. Y. Nishina and N. Kuroda, *Physica B* **99,** 357 (1980).
3. K. Schubert, "Kristallstrukturen zweikomponentiger Phasen," Springer-Verlag, Berlin/New York (1964).
4. G. C. Vessoli, *Mater. Res. Bull.* **6,** 1201 (1971).
5. H. Iwasaki, Y. Watanabe and S. Ogawa, *J. Appl. Crystallogr.* **7,** 611 (1974).
6. W. J. Duffin and J. H. C. Hogg, *Acta Crystallogr.* **20,** 566 (1966).
7. J. Kakinoki and Y. Komura, *Acta Crystallogr.* **19,** 137 (1965).
8. J. Rigoult, A. Rimsky, and A. Kuhn, *Acta Crystallogr. Sect. B* **36,** 916 (1980).
9. W. F. T. Pistorius, *Prog. Solid State Chem.* **11,** Pt. 1, 48 (1976).
10. N. Kuroda, Y. Nishina, H. Iwasaki, and Y. Watanabe, *Solid State Commun.* **38,** 139 (1981).
11. S. Inoue, private communication.
12. N. Kuroda and Y. Nishina, *Solid State Commun.* **28,** 439 (1978).
13. N. Kuroda and Y. Nishina, *Solid State Commun.* **38,** 139 (1981).
14. C. Carlone, S. Jandl, and H. R. Shanks, *Phys. Status Solidi B* **103,** 123 (1981).